HOSTED BY

ELSEVIER

Available online at www.sciencedirect.com

ScienceDirect

journal homepage: http://ees.elsevier.com/ejbas/default.asp

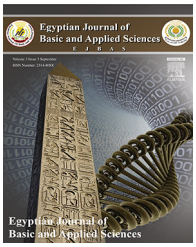

Full Length Article

Bivalent transition metal complexes of 3-(2-(4-(dimethylamino)benzylidene)hydrazinyl)-3-oxo-N-(thiazol-2-yl)propanamide: Structural, spectral, DFT, ion-flotation and biological studies

Rania Zaky *, *Ahmed Fekri*, *Yasmeen G. Abou El-Reash*, *Hany M. Youssef*, *Abdulrahman Y. Kareem*

Department of Chemistry, Faculty of Science, Mansoura University, Mansoura, Egypt

ARTICLE INFO

Article history:
Received 11 April 2016
Received in revised form 12 June 2016
Accepted 26 June 2016
Available online 4 July 2016

Keywords:
Schiff base
Spectroscopy
Computational
Ion-flotation
Biological activity

ABSTRACT

Co(II), Pb(II), Hg(II) and Cd(II) complexes of the 3-(2-(4-(dimethylamino)benzylidene)hydrazinyl)-3-oxo-N-(thiazol-2-yl)propanamide (H_2L) were synthesized. The prepared compounds were interpreted by elemental analysis: C, H, N, M, Cl; physical measurements as molar conductance; and magnetic susceptibility spectroscopic techniques as IR, UV–visible, ^{1}H NMR, MS spectra. The computational studying was estimated to approve the geometry of the isolated solid compounds. Also, Pb(II) and Cd(II) were separated using a simple, rapid and inexpensive quantitative flotation method prior to their determinations using atomic absorption spectrophotometric (AAS). The main parameters influencing the flotation process were examined (ca. initial pH, metal ion, surfactant and ligand concentrations, presence of foreign ions, and temperature). Furthermore, the biological activity (antimicrobial, antioxidant and cytotoxic) of the investigated compounds was tested.

1. Introduction

Heterocyclic systems containing thiazole moiety are very interesting compounds where sulfur drugs, biocides, fungicides, dyes and chemical reaction accelerators are synthesized from 2-aminothiazoles. Also, this moiety is a very good complexing agent that provides several probable binding sites for complexation of diverse metal ions. Schiff-bases of 2-amino thiazoles and their transition metal complexes play an important role in pharmaceutical chemistry along with co-ordination chemistry [1–5].

Furthermore, Schiff-bases as selective metal extracting agents were utilized in analytical chemistry in addition to spectroscopic determination of some transition metal ions, where many separation/preconcentration techniques (ion-flotation, ion-selective electrode, solid phase extraction, co-precipitation, column extraction, cloud point extraction and liquid–liquid

* *Corresponding author.*
E-mail address: rania.zaky@yahoo.com (R. Zaky).
http://dx.doi.org/10.1016/j.ejbas.2016.06.004

extraction) were stated to determine trace metal [6–10]. Ion-flotation method attracted a significant attention because it was simple, cheap, highly efficient, and a rapid quantitative method [11–14].

In extension of our work on Schiff-bases of 2-amino thiazoles [15–19], the purpose of the current work was the preparation and characterization of isolated solid complexes Co(II), Pb(II), Hg(II) and Cd(II) with H_2L. The mode of complexes was explained on the basis of many spectroscopic techniques. Also, the biological activity (antimicrobial, antioxidant and cytotoxic) of the investigated compounds was tested.

2. Experimental

2.1. Materials and reagents

The materials used were pure (Sigma, Aldrich, or Merck). They involved (a) organic substance such as as 3-hydrazinyl-oxo-N-(thiazole-2-)propanamide and 4-dimethylamino-benzaldehyde, oleic acid (HOL); (b) metal salts such as $[Co(CH_3COO)_2].4H_2O$, $[CdCl_2].2H_2O$, $Pb(NO_3)_2$, and $HgCl_2$; (c) solvent such as diethyl ether, dimethyl formamide, and dimethyl absolute ethyl alcohol.

2.2. Solutions

Stock solution of oleic acid (HOL) (6.36×10^{-2} mol.L^{-1}) was prepared by dispersing 20 mL in one liter of kerosene. Also, stock solutions of $[CdCl_2].2H_2O$ and $Pb(NO_3)_2$ (1×10^{-2} mol.L^{-1}) were prepared in double distilled water. A 1×10^{-2} mol.L^{-1} stock solutions of H_2L was prepared in absolute ethyl alcohol.

2.3. Instrumentation

- The FTIR spectrophotometer "Mattson 5000, Madison, USA" in the range 4000–400 cm^{-1} was used to record the infrared spectra of the ligand and its complexes in KBr disks.
- The "EM-390 (200 MHz) on a Varian Mercury-300 instrument (Switzerland)" was used to detect the ^{1}H NMR spectra of the ligand, Hg(II) and Cd(II) complexes.
- The "Mattson 5000 FTIR spectrophotometer" was used to record the mass spectra.
- The magnetic susceptibility balance "Johnson Matthey Wayne, Pennsylvania, USA" with $Hg[Co(SCN)_4]$ as calibrant was used to evaluate the magnetic moment values at room temperature (25 ± 1 °C).
- The "Shimadzu UV 240 (P/N 204–58000) spectrophotometer (USA) in the range 200–900 nm" was used to record the electronic spectra of the complexes in DMSO.
- GBC, SensAA Series Atomic Absorption Spectrometry (computerized AAS) with air-acetylene flame was used for the determinations of analyte under the optimum instrumental conditions (228.8 nm as wave length, 0.2–1.8 ppm as working calibrating range with 0.009 μg/mL sensitivity for Cd(II), 217 nm as wave length, and 2.5–10 ppm as working calibrating range with 0.06 μg/mL sensitivity for Pb(II).
- Two types of cells were used in the flotation and separation experiments, which are cylindrical tube of (29, 45) cm in length and (1.2, 6) cm inner diameter with a stopper at the top.
- The "Hanna instrument 8519 digital pH meter" was used for the pH measurements.
- The "Perkin-Elmer 2400 Series II Analyzer" was used to determine the percentage of C, H and N in the synthesized compounds (Table 1).
- The standard methods were used to determine the metal contents in the complexes [20].

2.4. Synthesis of H_2L

The ligand was prepared by mixing equimolar amounts of 3-hydrazinyl-oxo-N-(thiazole-2-)propanamide (0.01 mol; 2 g) and 4-Dimethylamino-benzaldehyde (0.01 mol; 1.5 g), in 50 mL ethanol with 1 mL acetic acid glacial. The ligand was precipitated during reflux (3 hrs) and then separated by filtration followed by recrystallization from absolute ethyl alcohol and finally dried in a vacuum desiccator over anhydrous $CaCl_2$. The pureness of the compounds was tested by TLC (Scheme 1).

2.5. Synthesis of metal complexes

The solid complexes were prepared by reflux equimolar amounts of H_2L (3.31; 10.0 mmol) and 10.0 mmol of cobalt (II),

Table 1 – Elemental analysis and physical data of H_2L and its metal complexes.

Compound	Empirical formula molecular mass % found (calculated)	Color	M.P. (°C)	Yield %	%Found (calculated)					Λ_m*
					C	H	N	M	Cl	
H_2L	$C_{15}H_{17}O_2N_5S$ 331.349 (331.353)	Pale yellow	192	80	54.17 (54.37)	4.99 (5.17)	21.17 (21.14)	–	–	–
$[Co(HL)_2]$	Co $C_{30}H_{32}O_4N_{10}S_2$ 719.617 (719.620)	Brown	>300	75	50.17 (50.07)	4.52 (4.48)	19.50 (19.47)	8.22 (8.19)	–	6
$[Hg(HL)(H_2O)_2Cl]$	Hg $C_{15}H_{20}O_4N_5S$ Cl 602.411 (602.415)	Yellowish white	220	90	29.87 (29.91)	3.26 (3.35)	11.38 (11.63)	33.27 (33.30)	5.81 (5.89)	9
$[Cd(HL)_2]$	Cd $C_{30}H_{32}O_4N_{10}S_2$ 773.092 (773.090)	Yellowish white	>300	75	46.68 (46.61)	4.21 (4.17)	18.06 (18.12)	14.48 (14.54)	–	4
$[PbL(H_2O)_3]$	Pb $C_{15}H_{21}O_5N_5S$ 590.579 (590.582)	Yellowish white	>300	85	30.53 (30.51)	3.64 (3.58)	11.89 (11.86)	35.11 (35.08)	–	6

* In DMSO (Ohm^{-1} cm^2 mol^{-1}).

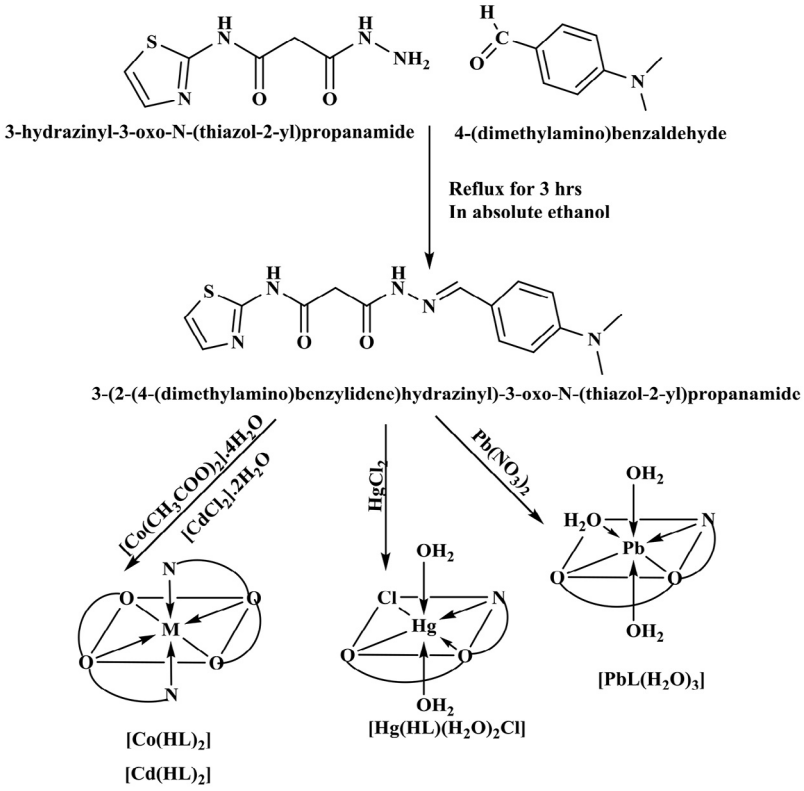

Scheme 1 – The outline of the synthesis of ligand (H_2L) and its metal complexes.

cadmium (II), lead (II), and mercury (II) salts. The mixture was refluxed for 1–3 h. The formed precipitate was filtered off and washed with hot ethanol and distilled water.

2.6. *Molecular modeling*

The DMOL3 program in Materials Studio package [21,22] was used to evaluate the cluster calculations. The simulations of geometry optimization of the isolated solid compounds were carried out using the density functional theory (DFT) *via* the GAUSSIAN 09 program package. The DNP basis sets are of analogous class to 6-31G Gaussian basis sets [23]. The DNP basis sets are more precise than Gaussian basis sets of identical size [24]. Based on the generalized gradient approximation (GGA), the RPBE functional [25] was considered the most excellent exchange-correlation functional [26]. The geometric optimization is carried out without any regularity restraint.

2.7. *Biological activity*

2.7.1. *Antibacterial and antifungal activities in terms of minimum inhibitory concentration*

- The MIC of the synthesized compounds was determined by applying agar streak dilution method [27].
- The strains involved *Staphylococcus aureus* and *Bacillus subtilis* as Gram (+) bacteria; *Escherichia coli* and *Pseudomonas aeruginosa* Gram (–) bacteria; and *Candida albicans* and *Aspergillus flavus* as fungi.
- For anti-bacterial the Ciprofloxacin (100 μg/mL) was used as standard, but Fluconazole (100 μg/mL) was used as standard for anti-fungal.
- A stock solution (100 μg/mL) of the examined compounds in DMSO was prepared and then incorporated in specified quantity of molten sterile.
- A certain amount of the medium containing tested compound was decanted into a Petri dish to reach a depth of 3–4 mm at 40–50 °C and then allowed to solidify.
- The micro-organism suspension was set to take about 105 cfu/mL and smeared to plates with diluted compounds in DMSO to be tested and then incubated for 24–48 h at 37 °C.
- The MIC was measured until the lowest concentration of the test substance showed no visible growth of bacteria or fungi on the plate.

2.7.2. *Anti-oxidant activity screening assay*

2.7.2.1. *Anti-oxidant activity screening assay – ABTS method.*

- In ABTS method, 2 mL of ABTS (2, 2′-azinobis-(3-ethylbenzothiazoline-6-sulfonic acid)) solution (60 mM), 3 mL MnO_2 solution (25 mg/mL) and 5 mL aqueous phosphate buffer solution (pH 7, 0.1 M) were added to tested compounds.
- The mixture was shaken, centrifuged, filtered and then the absorbance was measured at λ734 nm of the resultant green–blue solution (ABTS radical solution).
- Then, 50 mL of the tested compounds (2 mM) in spectroscopic grade methanol/phosphate buffer (1:1) was added.

- The absorbance was detected and the color intensity reduction was expressed as % inhibition. The standard antioxidant L-ascorbic acid was used as a positive control.
- Blank sample was run without ABTS and using methanol/phosphate buffer (1:1) in place of tested compounds. However, the ABTS and methanol/phosphate buffer (1:1) was used as a negative control [28,29].

$$I\% = (A_{blank} - A_{sample})/(A_{blank}) \times 100$$

where A_{blank} is the absorbance of the control reaction, and A_{sample} is the absorbance in the presence of the samples or standards.

2.7.2.2. *Anti-oxidant screening assay for erythrocyte hemolysis*. By cardiac puncture the blood was collected in heparinized tubes. Erythrocytes were obtained from plasma and the buffy coat. Then, it was washed by NaCl (0.15 M) three times. Then, at 2500 rpm the erythrocytes were centrifuged to attain a regularly packed cell for 10 min. In this assay system erythrocyte hemolysis was mediated by peroxyl radicals [30]. To test the samples at various concentrations a 10% suspension of erythrocytes in pH 7.4 PBS was added to the identical volume of 200 mM of AAPH solution. Then the reaction mixture was shaken and incubated at 37 °C for one hour. After this, the mixture was detached, diluted with PBS (eight volumes) and centrifuged at 2500 rpm for 10 min. The absorbance (A) of the supernatant was detected at 540 nm. As well, eight volumes of distilled water were added to the mixture to achieve whole hemolysis, and then at 540 nm the absorbance (B) of the supernatant was achieved after centrifugation was measured. The % hemolysis was determined *via* the following equation:

$$\%\ \text{hemolysis} = (1 - A/B) \times 100\%$$

2.7.2.3. *Cell proliferation assay*.

- The inhibitory effects of compounds on cell growth were determined by MTT colorimetric assay [31,32].
- The antibiotics used were 100 units/mL penicillin + 100 μg/mL streptomycin at 37 °C under 5% CO_2 for 48 h incubator and seeds in a 96-well plate with density 1.0×10^4 cells/well [33,34].
- Then a different concentration of compounds was conserved into the incubated cells for 24 h. After 24 h, 20 μL of MTT solution at 5 mg/mL was added and incubated for 4 h.
- Then DMSO in volume of 100 μL was added to each well to dissolve the purple formazan. By using a plate reader (EXL 800, USA) the colorimetric test was determined at absorbance of 570 nm.
- The % of relative cell viability was determined by using the following equation:

$$\text{A570 of treated samples/A570 of untreated sample} \times 100$$

2.7.2.4. *Flotation–separation procedure*. A definite amount of Cd(II) or Pb(II) solutions, quantified for each investigation process, was mixed with a solution of prepared ligand. The pH of previous mixture was adjusted with HNO_3 and/or NaOH to the desired value. Then, the solution was invented to 10 mL with double distilled water, and then the cell was shaken well for 2 min to ensure complete complexation. After this, 2 mL of surfactant (HOL with known concentration) was added and the cell was then inverted upside down strongly twenty five times by hand and was left for five minutes standing for complete flotation. Finally the concentration of Cd(II) or Pb(II) ions that remained in the mother liquor was analyzed *via* AAS. The floatability (F %) of Cd(II) or Pb(II) ions was calculated according to the following relation:

$$F\% = (C_i - C_f)/Ci \times 100$$

where C_i and C_f are the initial and the final concentrations of Cd(II) or Pb(II) ions in the mother liquor, respectively.

3. Results and discussion

3.1. *IR and mass spectra*

The H_2L and its metal complexes' significant infrared bands were taken to detect the influence of a metal bonding on the ligand vibration in the solid complexes. The ligand IR spectrum showed a medium-intensity broad bands due to $\upsilon(NH)_1$, $\upsilon(NH)_2$ and $\upsilon(CH_2)$ at 3200, 3174 and 3089 cm^{-1} [35], respectively. Also, there are three sharp bands observed due to $\upsilon(C{=}N)$ [36], $\upsilon(C{=}O)_1$ and $\upsilon(C{=}O)_2$ [37] at 1605, 1688 and 1667 cm^{-1}, respectively (Table 2). Also, the MS of H_2L displayed the molecular ion peak $[M]^+$ of H_2L at m/z = 331.342 (34.28%) which is equal to its molecular weight and relating to the moiety of the ligand [($C_{15}H_{17}O_2N_5S$) atomic mass 331.353 u] (Fig. 1).

In the IR spectra of $[Co(HL)_2]$, $[Hg(HL)(H_2O)_2Cl]$ and $[Cd(HL)_2]$ complexes, H_2L behaved as a mononegative tridentate ligand coordinating *via* (C═N), carbonyl oxygen $(C{=}O)_1$ and $(C{=}O{-})_2$. This chelation mode was maintained by (i) the disappearance of $\upsilon(C{=}O)_2$ and $\upsilon(NH)_2$ with immediate entrance of new bands at 1603–1611 and 1065–1189 cm^{-1} which is attributable to $\upsilon(C{=}N)^*_2$ and $\upsilon(=C{-}O)_2$ (enolic) respectively [38], (ii) the shift of azomethine nitrogen $\upsilon(C{-}N)$ and $\upsilon(C{-}O)_1$ to lower wave numbers and (iii) the presence of novel bands in the 521–524 and 460–486 cm^{-1} region which is ascribed to $\upsilon(M{-}O)$and $\upsilon(M{-}N)$, respectively [39].

Also, the IR spectrum of $[PbL(H_2O)_3]$ complex showed that H_2L acted as a binegative tridentate ligand coordinating *via* (C═N) and $(=C{-}O{-})_1$ $(=C{-}O{-})_2$. This mode was proposed by (i) the shift of (C═N) to lower wavenumber, (ii) the disappearance of $\upsilon(C{=}O)_1$, $\upsilon(C{=}O)_2$, $\upsilon(NH)_1$ and $\upsilon(NH)_2$ with instantaneous appearance of new band at 1624, 1605, 1179 and 1124 cm^{-1}, which is attributable to $\upsilon(C{=}N)^*_1$, $\upsilon(C{=}N)^*_2$, $\upsilon(=C{-}O)_{1(enolic)}$ and $\upsilon(=C{-}O)_{2\ (enolic)}$, respectively, and (iii) the appearance of new bands at 521 and 423 cm^{-1} which may be ascribed to $\upsilon(M{-}O)$and $\upsilon(M{-}N)$ respectively [39].

3.2. *Nuclear magnetic resonance spectral studies*

In H_2L and its Hg(II) and Cd(II) complexes ^1H NMR spectra were detected in DMSO. There are two signals at 11.27 and 12.23 ppm attributed to the protons of $(NH)_1$ and $(NH)_2$, respectively, in the spectrum of H_2L (Fig. 2). In 6.60–8.04 ppm region multiplet signals

Table 2 – Most important IR spectral bands of H_2L and its metal complexes.

Compound	$\upsilon(NH)_1$	$\upsilon(NH)_2$	$\upsilon(CH_2)$	$\upsilon(C{=}O)_1$	$\upsilon(C{=}O)_2$	$\upsilon(C{=}N)$	$\upsilon(C{=}N)^*_1$	$\upsilon(C{=}N)^*_2$	$\upsilon(C{=}O)_{1(enolic)}$	$\upsilon(C{=}O)_{2(enolic)}$	$\upsilon(M{-}O)$	$\upsilon(M{-}N)$
H_2L	3200	3174	3089	1688	1667	1605	–	–	–	–	–	–
$[Co(HL)_2]$	3239	–	3087	1664	–	1583	–	1608	–	1125	521	486
$[Hg(HL)(H_2O)_2Cl]$	3192	–	3067	1670	–	1596	–	1611	–	1189	524	460
$[Cd(HL)_2]$	3225	–	3080	1669	–	1591	–	1605	–	1129	521	470
$[PbL(H_2O)_3]$	–	–	3085	–	–	1589	1624	1605	1179	1124	521	423

were observed related to the —N═C**H**— and aromatic protons. At 3.46 and 3.79 ppm there are two sharp singlet related to active methylene protons (—C**H**$_2$) and ph–N—(C**H**$_3$)$_2$, respectively. Also, the ^{1}H NMR spectra of the Cd(II) and Hg(II) complexes showed the signal ascribed to the $(NH)_1$ and proton representing that these group played no part in coordination. But the absence of signal due to $(NH)_2$ proton gave emphasis to the deprotonation of the enolized carbonyl oxygen (—C═O)$_2$.

3.3. *Magnetic moments and electronic spectra*

The electronic spectrum of $[Co(HL)_2]$ complex showed two bands at 20 618 and 16 949 cm^{-1} ascribed to $^4T_1g \rightarrow {}^4A_2g$ (F) and $^4T_1g \rightarrow {}^4T_1g$ (P) transitions, respectively, in an octahedral configuration [40]. The calculated values of *Dq*, *B*, β and υ_2/υ_1 values are in good promise with those informed for octahedral Co(II) complexes. The position of υ_1 (7901 cm^{-1}) was calculated theoretically [40]. Also, the values of the magnetic moments value (μeff. = 5.0 BM) are reliable with octahedral geometry around the Co(II) ion.

3.4. *Geometry optimization with DFT method*

The design of new molecular compounds can be recognized by applying computational chemistry tools, which is a potent protocol for interpreting their stabilities and calculated lots of structural parameters for multidentate Schiff base ligand (Table 3).

DFT calculations are performed to predict the host–gust interaction between the Schiff base and various metal cations. The molecular structure beside atom numbering of H_2L and its metal complexes is presented in Structure 1.

3.4.1. *Molecular parameters*

The Quantum chemical parameters (the energies of the HOMO and LUMO) of investigated compounds were attained. Also, the total energy, binding energy, spin polarization energy, exchange-correlation energy, electrostatic energy, kinetic energy, sum of atomic energy and dipole moment were calculated (Table 3). From the attained data we can assumed that:

1. The energies of the HOMO and LUMO are negative values, which showed the stability of isolated complexes (Fig. 3).
2. The lower EHOMO values point to the molecule donating electron ability is frailer. On contrasting, the greater HOMO energy recommended that the molecule is a decent electron donor.
3. The binding energy of complexes was higher than free ligand, which indicated great the stability of the isolated solid complexes.
4. The free ligand showed higher values of dipole moment than the isolated solid complexes that improved the potent activities of the free ligands.

3.4.2. *Molecular electrostatic potential (MEP) of H_2L*

The MEP was considered a good descriptor for decisive sites for electrophilic and nucleophilic attack [41]. In the present study, 3D plots of MEP were drawn for the ligand and their metal complexes (Fig. 4). Based on the MEP, one can generally order the electron-rich area which has red color on the map (favor

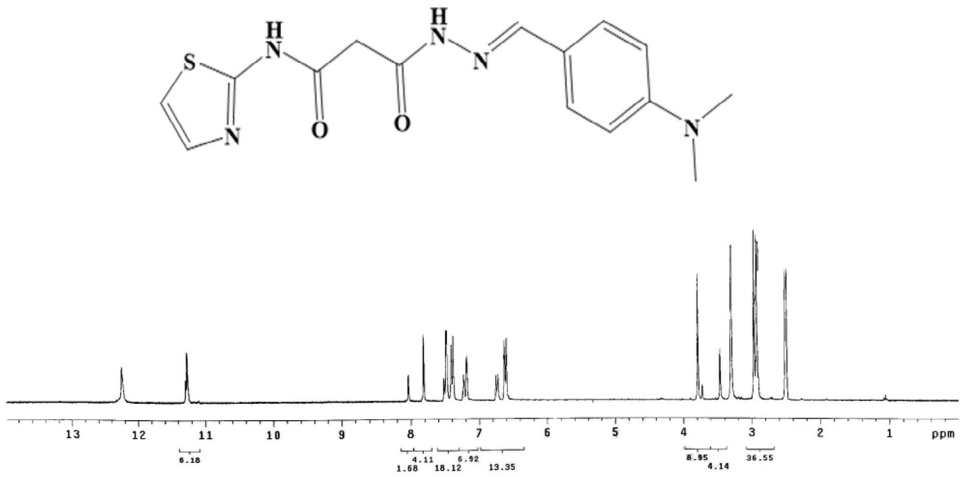

Fig. 1 – ^{1}H NMR spectrum of 3-(2-(4-(dimethylamino)benzylidene)hydrazinyl)-3-oxo-*N*-(thiazol-2-yl)propanamide in DMSO.

site for electrophilic attack). However, the electron-poor region has blue color (favor site for nucleophilic attack) [42]. But the region with green color points to neutral electrostatic potential region.

3.5. *Biological activity*

The Schiff bases' biological activity stimulated us to assume systematic studies on their complexation affinity and test their abilities against economically vital fungi and bacteria [43,44].

3.5.1. *Antifungal activity*

The results showed that the ligand and its metal complexes have significant activity against *Candida albicans and Aspergillus flavus* (Table 4). The ligand (H_2L) and $[Co(HL)_2]$ complex were more effective against *Aspergillus flavus* than *Candida albicans* in comparison with the Fluconazole as standard drug [45].

3.5.2. *Antibacterial activity*

The investigated compounds along with Ciprofloxacin (standard drug) and DMSO (solvent control) were screened separately for their antibacterial activity [46–48]. The activity of the tested compounds was compared to the activity of Ciprofloxacin as a standard antibiotic. The MIC values showed that H_2L and $[Co(HL)_2]$ complex have the highest antibacterial activity (Table 5).

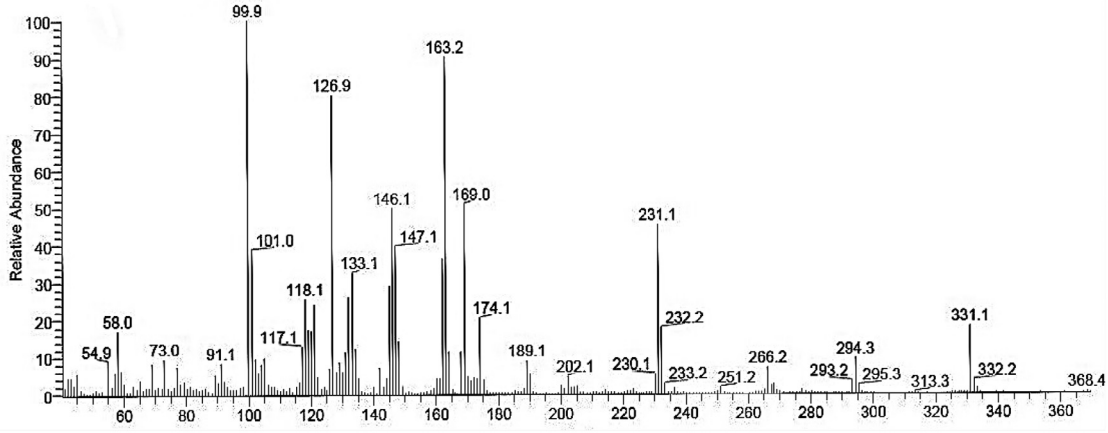

Fig. 2 – Mass spectra of 3-(2-(4-(dimethylamino)benzylidene)hydrazinyl)-3-oxo-*N*-(thiazol-2-yl)propanamide.

Table 3 – The molecular parameters of the ligand and its complexes.

Compound	Total energy (Ha)	Binding energy (Ha)	Dipole moment (debye)	HOMO eV	LUMO (eV)
H_2L	−1404.622293	−6.9256921	8.5025	−4.719	−2.096
$[Co(HL)_2]$	−2975.879536	−14.6804663	10.4731	−3.801	−2.716
$[Hg(HL)(H_2O)_2Cl]$	−2246.291573	−8.1242131	4.8789	−4.947	−2.644
$[Cd(HL)_2]$	−2897.959614	−13.6468858	5.4398	−4.482	−2.011
$[PbL(H_2O)_3]$	−1754.309944	−8.3909023	8.0227	−4.998	−2.853

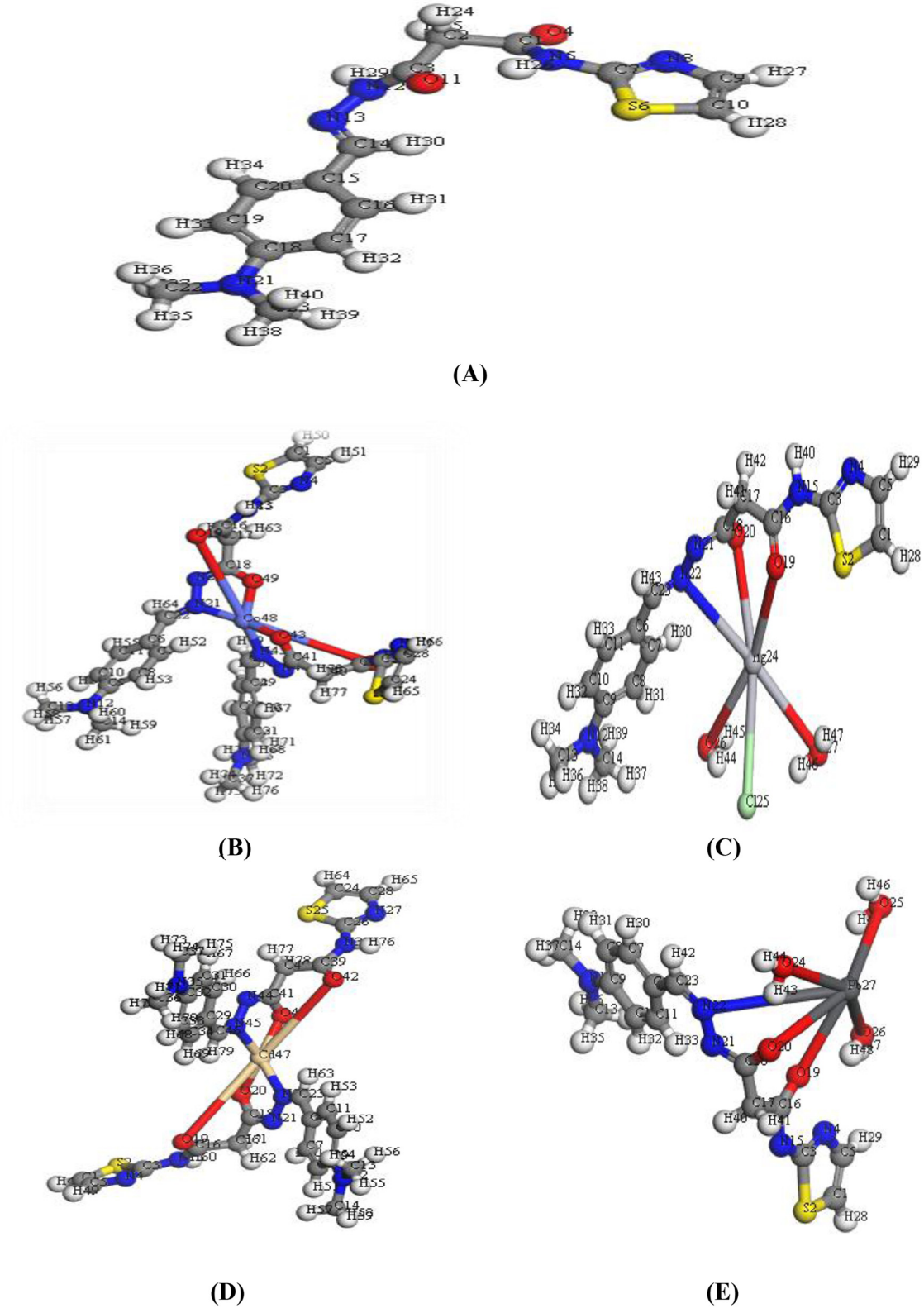

Structure 1 – Molecular modeling of (A) H_2L, (B) $[Co(HL)_2]$, (C) $[Hg(HL)(H_2O)_2Cl]$, (D) $[Cd(HL)_2]$, and (E) $[PbL(H_2O)_3]$.

3.5.3. *The antioxidant activity of ligand and its metal complexes*

The antioxidant rank of prepared compounds was measured using ABTS assay [49]. All tested compounds have low anti-oxidant activity in comparison with complex $[Co(HL)_2]$, which displayed the maximum antioxidant activity in comparison with standard ascorbic-acid. Moreover, the anti-oxidant activity of prepared compounds was tested for erythrocyte hemolysis. All

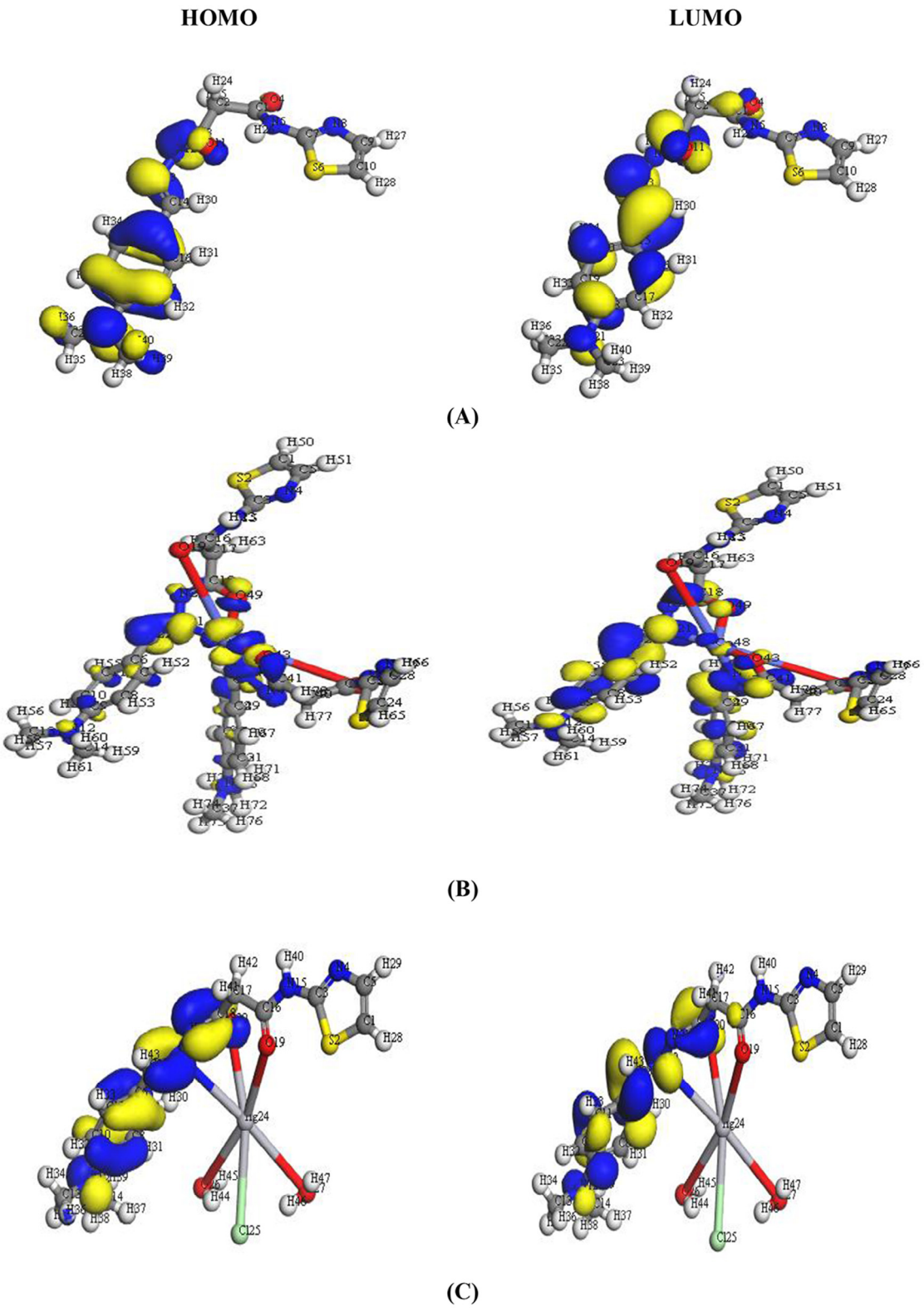

Fig. 3 – The HOMO and LUMO of (A) H_2L, (B) $[Co(HL)_2]$, (C) $[Hg(HL)(H_2O)_2Cl]$, (D) $[Cd(HL)_2]$, and (E) $[PbL(H_2O)_3]$.

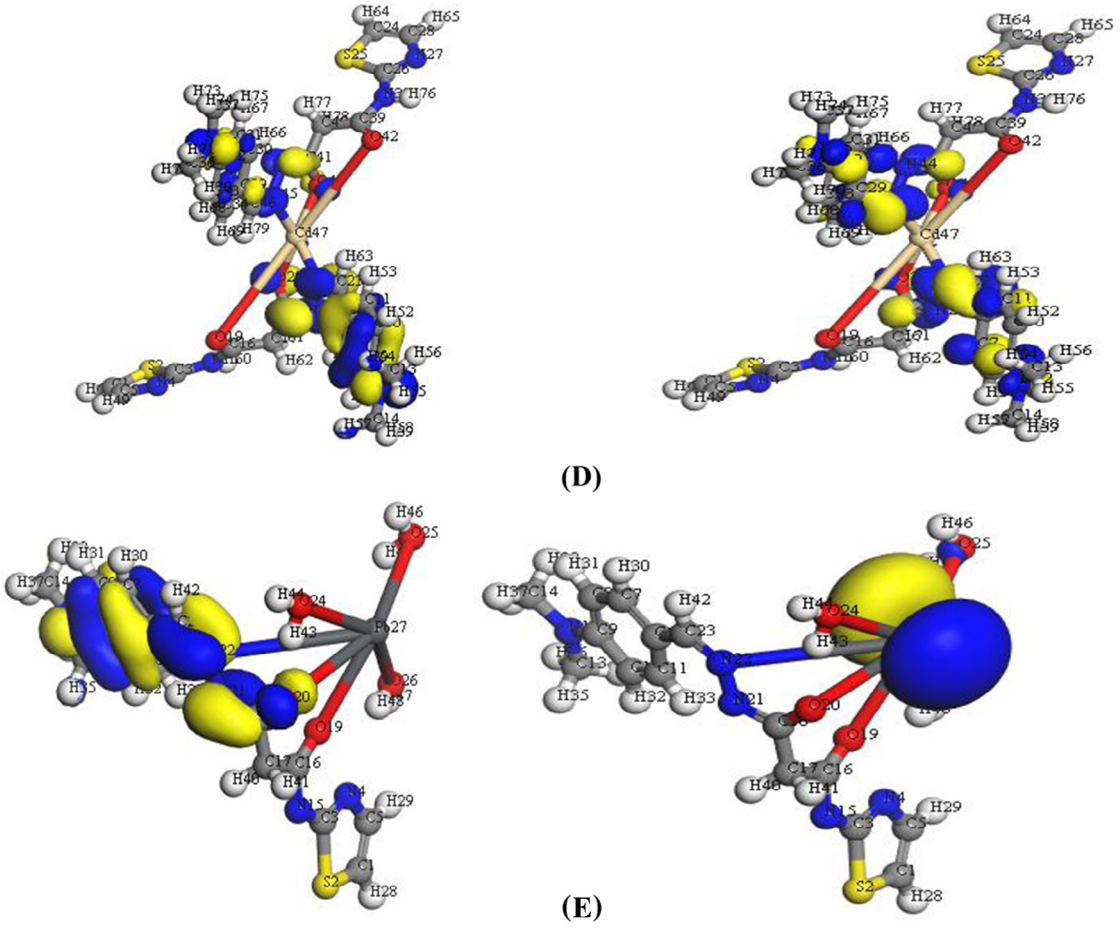

Fig. 3 – (*continued*)

the tested compounds demonstrated weak anti-oxidative activity in the hemolysis assay, but $[Co(HL)_2]$ gave better results (Tables 6 and 7). The significant antioxidant activity was attributable to the existence of two carbonyl (C═O) and azomethine (C═N) groups.

3.5.4. *The cytotoxicity of H_2L and its metal complexes on HCT-116 cell line*

The cytotoxicity assays of H_2L and its metal complexes against human colorectal carcinoma cells lines (HCT) are illustrated in Table 8. The data observed that $[Co(HL)_2]$ (IC50 = 11.4 μM) demonstrated a much higher inhibitory effect than the other isolated compounds. However, $[Hg(HL)(H_2O)_2Cl]$ complex which has higher IC50 value (>100 μg/mL) showed nearly no activity [50].

3.6. *Ion-flotation separation*

3.6.1. *Influence of initial pH*

Some experiments were conducted to study the effect of the pH of a solution on the floatability of 2×10^{-4} mol L^{-1} of metal ions using 2×10^{-4} mol L^{-1} of prepared ligand and 1×10^{-3} mol L^{-1} of HOL. The results showed that higher floatability was detected at the pH range of 5–9 for Cd(II) and 6–9 for Pb(II) ions (Fig. 5). This eases the ability to apply the prepared ligand for the separation of metal ions from different media. Hence, pH ~7 was fixed for further experiments.

3.6.2. *Influence of initial metal concentration*

Efforts to float different concentrations of Pb(II) and Cd(II) ions were carried out with 2×10^{-4} mol L^{-1} ligand (H_2L) + 1×10^{-3} mol L^{-1} HOL at pH~7. The maximum flotation efficiency of Cd(II) and Pb(II) ions was determined for the prepared ligand whenever the ratio of M:L is (1:1) (Fig. 6). The chelating agent gave quantitative separation of Cd(II) and Pb(II) ions (~100%), which may be ascribed to the presence of sufficient amounts of prepared ligand to bind all Cd(II) and Pb(II) ions. Therefore, the ratio of M:L of 1:1 was used throughout.

3.6.3. *Influence of ligand concentration*

The collecting ability of prepared ligand toward Cd(II) and Pb(II) ions was tested to show the effect of different concentrations of prepared ligand on the floatability of the analytes using 1×10^{-3} mol L^{-1} HOL at pH~7. The data revealed that the floatability of Cd(II) and Pb(II) ions increases sharply reaching its maximum value at M:L ratio of 1:1 (Fig. 7). Excess ligand has no adverse effect on the flotation process, and accordingly 2×10^{-4} mol L^{-1} of prepared ligand was used throughout.

3.6.4. *Influence of surfactant concentration*

Several trials were examined to float Cd(II) and Pb(II) ions with surfactants only, but the maximum recovery received was 43%. Thus, extra series of experiments were done to float 2×10^{-4} mol L^{-1} Cd(II) and Pb(II) ions in the presence of

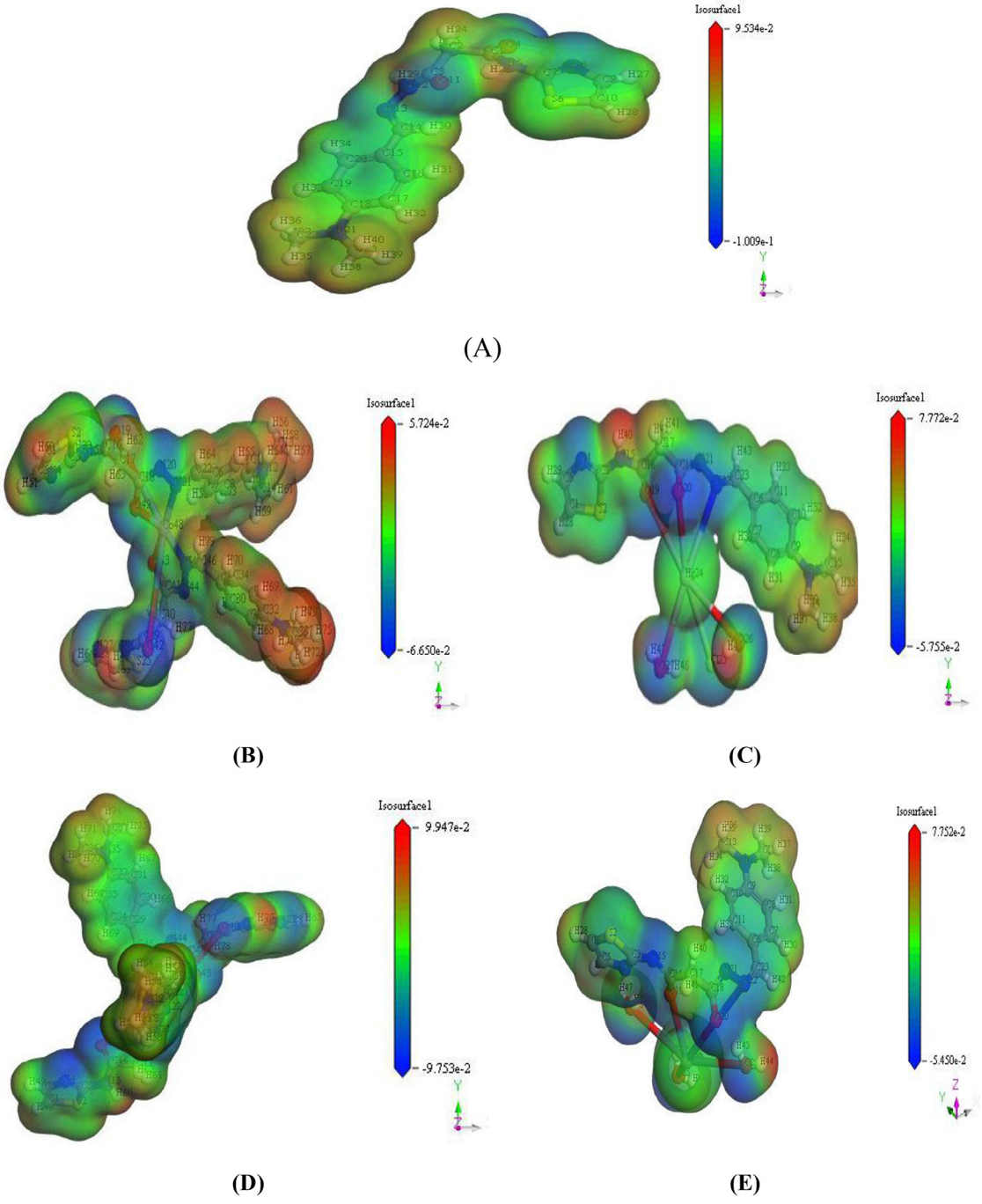

Fig. 4 – Molecular electrostatic potential map for (A) H_2L, (B) $[Co(HL)_2]$, (C) $[Hg(HL)(H_2O)_2Cl]$, (D) $[Cd(HL)_2]$, and (E) $[PbL(H_2O)_3]$.

2×10^{-4} mol L^{-1} of H_2L and various concentrations of HOL (1×10^{-3}–5×10^{-2} mol L^{-1}) at pH~7. The results proved that the high floatation % of Cd(II) and Pb(II) ions was achieved in the concentration range 1×10^{-3}–9×10^{-3} mol L^{-1} of HOL (Fig. 8).

It was noticed that; the incomplete separation of Cd(II) and Pb(II) ions at higher surfactant concentration regarding to the fact that; the addition of surfactant led to change in the state of formed complexes from coagulated precipitate to re-dispersion through coagulation flotation. Furthermore, at high surfactant concentration, the poor flotation resulted from the

Table 4 – Antifungal activities in terms of MIC (μg/mL).

Compound	*C. albicans*	*A. flavus*
Fluconazole	1.56	0.78
H_2L	4.68	3.12
$[Co(HL)_2]$	6.25	4.68
$[Hg(HL)(H_2O)_2Cl]$	>100	>100
$[Cd(HL)_2]$	>100	75
$[PbL(H_2O)_3]$	75	50

Table 5 – Antibacterial activities in terms of MIC (μg/mL).

Compound	Gram-negative		Gram-positive	
	E. coli	*P. aeruginosa*	*S. aureus*	*B. subtilis*
Ciprofloxacin	1.56	0.78	1.56	0.39
H_2L	9.37	6.25	4.68	2.34
$[Co(HL)_2]$	6.25	3.12	4.68	3.12
$[Hg(HL)(H_2O)_2Cl]$	>100	>100	>100	>100
$[Cd(HL)_2]$	75	37.5	50	75
$[PbL(H_2O)_3]$	25	18.75	37.5	37.5

formation of hydrated and stable envelope of surfactant on the air bubble surface or due to the formation of a hydrated micelle coating on the solid surface [51,52]. Consequently, increasing the hydrophobicity of the surface had an adverse effect on the flotation process. Thus, HOL with concentration of 1×10^{-3} mol L^{-1} was fixed throughout.

Table 6 – Anti-oxidant assays by ABTS method.

Method	ABTS	
	Abs(control)–Abs(test)/Abs(control)×100	
Compounds	Absorbance of samples	% inhibition
Control of ABTS	0.51	0
Ascorbic-acid	0.055	89.20
H_2L	0.156	69.40
$[Co(HL)_2]$	0.195	61.80
$[Hg(HL)(H_2O)_2Cl]$	0.306	40.00
$[Cd(HL)_2]$	0.258	49.40
$[PbL(H_2O)_3]$	0.256	49.80

Table 7 – Anti-oxidant assays by erythrocyte hemolysis.

Compounds	Erythrocyte hemolysis	
	A/B × 100	
	Absorbance of samples (A)	% hemolysis
Absorbance of H_2O (B)	0.896	–
Ascorbic-acid	0.042	4.70
H_2L	0.538	60.00
$[Co(HL)_2]$	0.293	23.70
$[Hg(HL)(H_2O)_2Cl]$	0.595	66.40
$[Cd(HL)_2]$	0.211	32.50
$[PbL(H_2O)_3]$	0.646	72.10

Table 8 – Cytotoxicity (IC50) of tested compounds on HCT-116 cell line.

Compounds	Cytotoxicity IC50 (μg/mL)
5-FU	5.2
H_2L	13.1
$[Co(HL)_2]$	11.4
$[Hg(HL)(H_2O)_2Cl]$	>100
$[Cd(HL)_2]$	37.5
$[PbL(H_2O)_3]$	20.1

IC50 (μg/mL): 1–10 (very strong), 11–20 (strong), 21–50 (moderate), 51–100 (weak) and above 100 (non-cytotoxic). 5-FU = 5-fluorouracil.

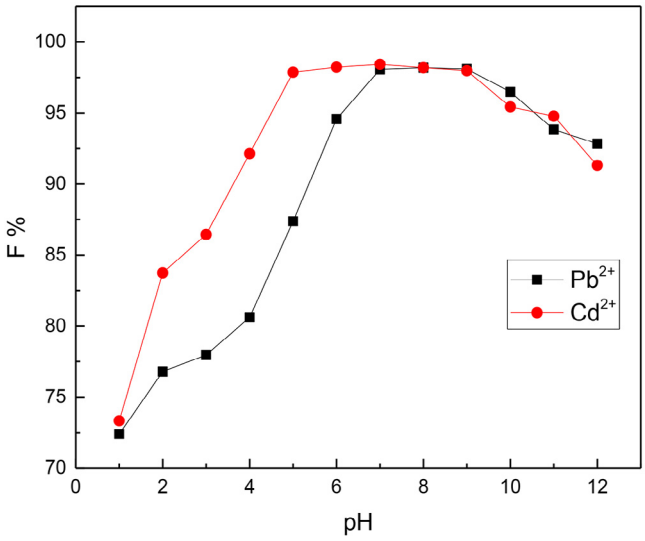

Fig. 5 – Influence of pH on the floatability of 2×10^{-4} mol.L^{-1} Cd(II) and Pb(II) ions using 2×10^{-4} mol.L^{-1} of ligand and 1×10^{-3} mol.L^{-1} HOL.

3.6.5. *Influence of temperature*

A series of experiments were done to test the floatation of Cd(II) or Pb(II) ions under a temperature range of 10–80 °C and the recommended conditions. For this purpose, a mixture containing Cd(II) or Pb(II) ions and H_2L and separated HOL solutions was either heated or cooled to the proposed temperature in a water bath. Then HOL solution was poured into Cd(II) or Pb(II) ions solution into the flotation cell, then jacketed with 1 cm thick fiberglass insulation and shaken well. According to results illustrated in Fig. 9, the decrease in separation efficiency by raising temperature over 80 °C may be due to increasing the

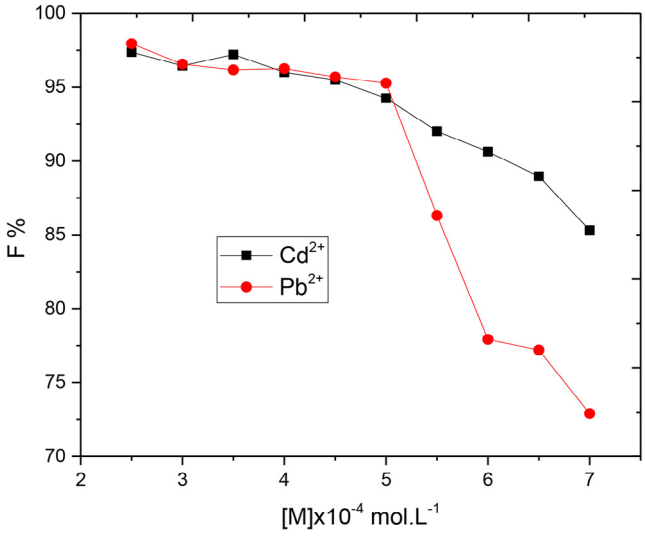

Fig. 6 – Floatability of different concentrations of Cd(II) and Pb(II) ions using 2×10^{-4} mol.L^{-1} of prepared ligand and 1×10^{-3} mol.L^{-1} HOL at pH ~7.

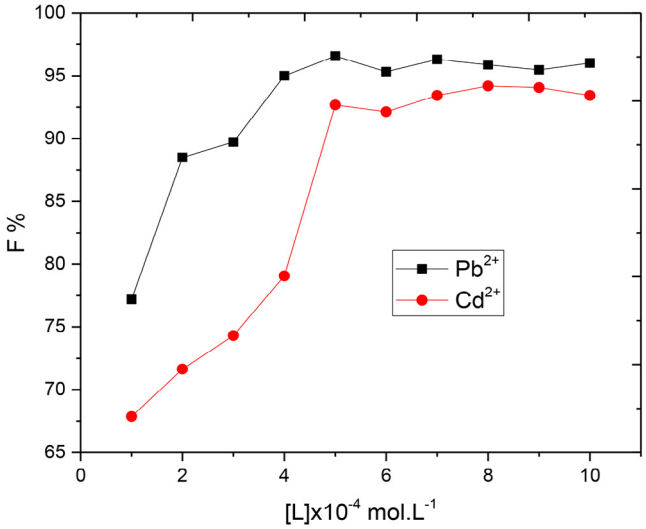

Fig. 7 – Floatability of 2×10^{-4} mol.L^{-1} Cd(II) and Pb(II) ions using different concentrations of prepared ligand and 1×10^{-3} mol.L^{-1} HOL at pH ~7.

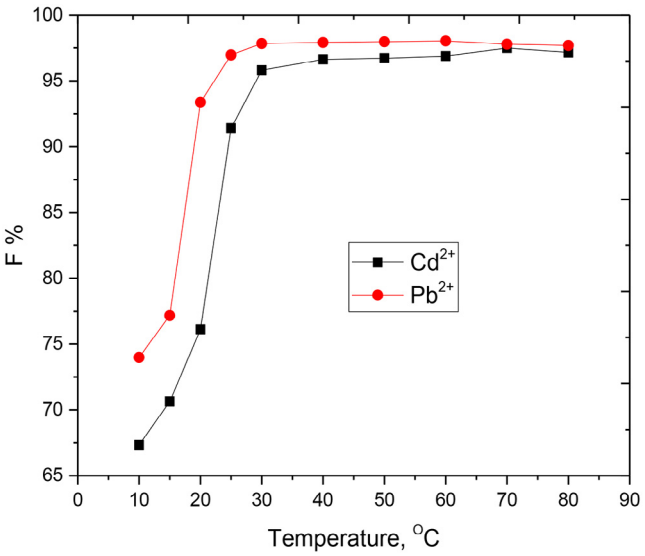

Fig. 9 – Floatability of 2×10^{-4} mol.L^{-1} Cd(II) and Pb(II) ions at different temperatures using 2×10^{-4} mol.L^{-1} of prepared ligand and 1×10^{-3} mol.L^{-1} HOL at pH ~7.

solubility of the precipitate and the instability of the foam raising the partial dissolution of the precipitate and decreasing the ability of foam to hold up the precipitate [53].

3.6.6. *Interference study*

The effect of foreign ions on the separation process is very important in order to investigate the ability of proposed method to be applied on real water samples. So the effect of various concentrations of both cations and anions, usually present in some water samples, on the removal percentage of 10 mg L^{-1} Cd(II) or Pb(II) ions at pH 7 and 30 mg L^{-1} H_2L was studied. Chloride salts of cations were used, whereas the anions were used as the corresponding potassium or sodium salts. The tolerable amounts of each ion, giving an error of ±4% in the removal efficiency of Cd(II) or Pb(II) ions, are listed in Table 9. It was proven that foreign ions with relatively high concentrations (in comparison with that of Cd(II) or Pb(II) ions) did not affect badly the flotation of cadmium or lead and the procedure can be applied on water samples.

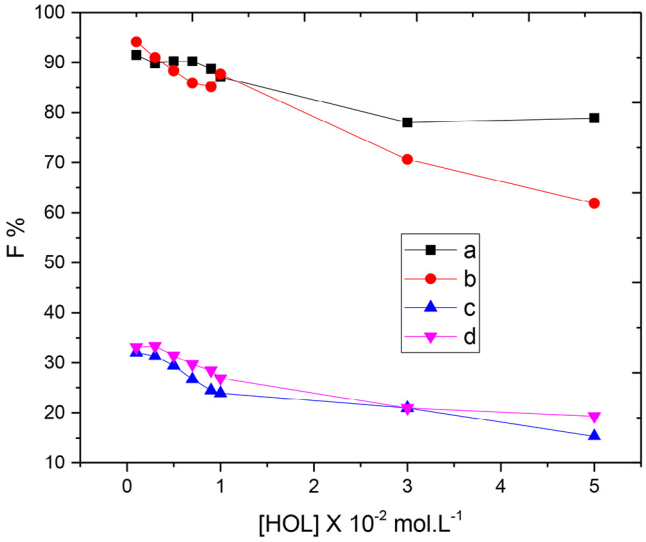

Fig. 8 – Floatability of 2×10^{-4} mol.L^{-1} Cd^{2+} (A and C) and Pb^{2+} (B and D) ions using different concentrations of HOL in the absence (C and D) and presence (A and B) of 2×10^{-4} mol.L^{-1} of prepared ligand at pH ~7.

3.6.7. *Application*

In order to inspect the applicability of the recommended procedure, a series of experiments were carried out to recover 10 mg L^{-1} of Cd(II) or Pb(II) ions spiked to 1 L of aqueous solution and some real water samples. Flotation experimentations were done using 50 mL clear, filtered, uncontaminated sample solutions at pH 7. The results showed that the recovery percentage was quantitative and agreeable under the recommended conditions of the applied flotation procedure (Table 10).

Table 9 – Effects of the foreign ions on the removal percentage of the examined metal ions.

Ion	Interference/analyte ratio (mg L^{-1})	Re % Cd(II)	Re % Pb(II)
Na^+	25	98.7	99.2
K^+	45	96.8	97.1
Mg^{2+}	35	97.4	97.9
Ca^{2+}	30	92.7	93.4
Cl^-	30	96.8	97.7
SO_4^{2-}	20	94.8	95.4
HCO_3^-	25	92.8	94.3
CH_3COO^-	40	94.5	95.4

[M = 2×10^{-4} mol.L^{-1}; Ligand = 2×10^{-4} mol.L^{-1}; HOL = 1×10^{-3} mol.L^{-1}; pH = 7].

Table 10 – Recovery of 15 mg L^{-1} of studied metal ions from some water samples.

Water samples (location)	Metal (mg L^{-1})	Re % Cd(II)	Re % Pb(II)
Sharm El-Sheikh	15	85.29064	96.64000
Alexandria	15	90.18719	97.29333
Wady	15	88.58128	98.95333
Mansoura	15	90.63054	97.69333

[Ligand = 2×10^{-4} mol.L^{-1}; HOL = 1×10^{-3} mol.L^{-1}; pH = ~ 7].

Table 11 – Different forms of oleic acid determined by spectrophotometric.

pH	(%)			Total
	HOL	Ol^-	NaOL	
5.2	100.0	0.0	0.0	100
8.0	6.5	34.2	0.0	100
8.2	38.5	57.7	3.8	100
9.0	13.6	68.2	18.2	100
11.5	0.0	80.0	20.0	100
12.0	0.0	52.2	47.8	100

3.6.8. *Suggested flotation mechanism*

The mechanism of the flotation of metal–ligand precipitates is suggested depending on the following points:

1. Cd(II) and Pb(II) reacted with the prepared ligand in a M:L ratio of 1:1 to give the complex M_2L according to the following equation:

$$M^{2+} + H_2L = M_2L + 2H^+$$

The prepared ligand has several sites comprising electronegative atoms, such as carbonyl oxygen (C═O) and azomethine nitrogen (C═N) as shown in Scheme 1.

2. Oleic acid began to dissociate at pH >5.2 [54] and the percentage of various forms of oleic acid is determined by IR analysis, and the data are presented in Table 11. The IR spectra of oleic acid with changing pH indicated that at 1300–1800 cm^{-1}, there are bands characteristic of the groups CO_2H, CO^{2-} and CO^{2-} contained with Na [55]. These data agree with those reported [56] that the C═O stretching band of oleic acid at 1705 cm^{-1} was shifted because of ionization to bands in the range 1520–1540 cm^{-1} for sodium oleate. As a result, oleic acid has the ability to interact with other systems, via hydrogen bond formation, either in its dissociated (R-COO-) or un-dissociated (R-COOH) forms depending on the pH of the medium and according to the following:

$$R\text{-}COOH + MHL^+ = R\text{-}COOH + LHM^+$$

$$R\text{-}COO^- + MHL^+ = R\text{-}COO^- + LHM^+$$

The combination of oleic acid surfactant with the cadmium–ligand or lead–ligand chelate gave hydrophobic aggregates that float with the help of air bubbles, which are created inside the flotation cell by shaking gently up to the surface of the solution [57].

4. Conclusions

In this paper, Co(II), Pb(II), Hg(II) and Cd(II) complexes of the 3-(2-(4-(dimethylamino)benzylidene)hydrazinyl)-3-oxo-N-(thiazol-2-yl)propanamide (H_2L) were synthesized and characterized by elemental analysis, spectroscopy techniques and physical measurements. The results showed that the H_2L acted as a mononegative or binegative tridentate ligand. Also, DFT calculations were done to predict the host–gust interaction between the Schiff base and various metal cations. Furthermore, the ligand and its complexes were screened for biological activity. The results show that the H_2L and Co(II) complex have highest biological activity. Also, it is successfully applied the recovery of Cd(II) or Pb(II) ions that obtained from different environmental water samples as shown in Table 10. The flotation mechanism was proposed dependent on the formation of hydrogen bonding between oleic acid surfactant and cadmium–ligand or lead–ligand complex.

REFERENCES

[1] Ortego L, Meireles M, Kasper C, Laguna A, Villacampa MD, Gimeno MC. Group 11 complexes with amino acid derivatives: synthesis and antitumoral studies. J Inorg Biochem 2016;156:133–44.
[2] Saini R, Kumar V, Gupta A, Gupta G. Synthesis, characterization, and antibacterial activity of a novel heterocyclic Schiff's base and its metal complexes of first transition series. Med Chem Res 2014;23:690–8.
[3] Zaky RR, Yousef TA, Abdelghany AM. Computational studies of the first order kinetic reactions for mononuclear copper(II) complexes having a hard–soft NS donor ligand. Spectrochim Acta A 2014;130:178–87.
[4] Raja S. Synthesis, spectroscopic characterization, analgesic, and antimicrobial activities of Co(II), Ni(II), and Cu(II) complexes of 2-[N,N-bis-(3,5-dimethyl-pyrazolyl-1-methyl)]aminothiazole. Med Chem Res 2015;24:1578–85.
[5] Ramalho TC, Martins TLC, Borges LEP, De Pinho MH, De Avillez RR, Da Cunha EFF. Influence of Zn–Cd substitution: spectroscopic and theoretical investigation of 8-hydroxyquinoline complexes. Spectrochim Acta A 2009;72:726–9.
[6] Wu Y, Jiang Z, Hu B, Duan J. Electrothermal vaporization inductively coupled plasma atomic emission spectrometry determination of gold, palladium, and platinum using chelating resin YPA4 as both extractant and chemical modifier. Talanta 2004;63:585–92.
[7] Qing Y, Hang Y, Wanjaul R, Jiang Z, Hu B. Adsorption behavior of Noble metal ions (Au, Ag, Pd) on nanometer-size titanium dioxide with ICP-AES. Anal Sci 2003;19:1417–20.
[8] Yin P, Xu Q, Qu R, Zhao G, Sun Y. Adsorption of transition metal ions from aqueous solutions onto a novel silica gel matrix inorganic-organic composite material. J Hazard Mater 2010;173:710–16.
[9] Chand R, Watari T, Inoue K, Kawakita H, Luitel HN, Parajuli D, et al. Selective adsorption of precious metal from hydrochloric acid solutions using porous carbon prepared from barley straw and rice husk. Miner Eng 2009;22:1277–82.
[10] Soylak M, Tuzen M. Coprecipitation of gold(III), palladium(II) and lead(II) for their flame atomic absorption spectrometric determinations. J Hazard Mater 2008;152:656–61.
[11] Ghazy SE, Mostafa HA, El-Farra SA, Fouda AS. Flotation-separation of nickel(II) from aqueous media using some

hydrazone derivatives as organic collectors and oleic acid as surfactant. Indian J Chem Techn 2004;11:787–92.
[12] Fu F, Qi W. Removal of heavy metal ions from wastewaters. J Environ Manage 2011;92:407–18.
[13] Ulewicz M, Walkowiak W, Bartsch R. Ion flotation of zinc(II) and cadmium(II) with proton-ionizable lariat ethers – effect of cavity size. Sep Purif Technol 2006;48:264–9.
[14] Polat H, Erdogan D. Heavy metal removal from waste waters by ion flotation. J Hazard Mater 2007;148:267–73.
[15] Ibrahim K, Zaky R, Gomaa E, El-Hady M. Spectral, magnetic, thermal studies and antimicrobial activity of (E)-3-(2-Benzylidenehydrazinyl)-3-oxo-N-(Thiazol-2-yl) propanamide complexes. Res J Pharm Biol Chem Sci 2011;2(3):391–404.
[16] Ibrahim K, Zaky R, Gomaa E, El-Hady M. The association and formation constants For $NiCl_2$ stoichiometric complexes with (E)-3-(2-benzylidene hydrazinyl)-3-oxo-N-(thiazol-2-yl)propanamide. Anaele Universitatii din Bucuresti 2011;20(2):149–54.
[17] El-Hady M, Zaky R, Ibrahim K, Gomaa E. (E)-3-(2-(furan-ylmethylene)hydrazinyl)-3-oxo-N-(thiazol-2yl)propanamide complexes: synthesis, characterization and antimicrobial studies. J Mol Struct 2012;1016:169–80.
[18] Ibrahim K, Gomaa E, Zaky R, El-Hady M. The association and formation constants for $CuCl_2$ stoichiometric complexes with (E)-3-(2-Benzylidene Hydrazinyl)-3-oxo-N-(thiazol-2-yl)propanamide in absolute ethanol solution 294.15 K. Am J Chem 2012;2(2):23–6.
[19] Ibrahim K, Zaky R, Gomaa E, El-Hady M. Physicochemical studies and biological evaluation on (E)-3-(2-(1-(2-hydroxyphenyl) hydrazinyl)-3-oxo-N-(thiazol-2yl)propanamide complexes. Spectrochimica Acta Part A 2013;107:133–44.
[20] Vogel A I. Quantitative inorganic analysis. London: Longmans; 1989.
[21] Delley B. Phys Rev 2002;65:85403–8509.
[22] Modeling and Simulation Solutions for Chemicals and Materials Research. Materials Studio (Version 5.0), Accelrys software Inc., San Diego, USA. <www.accelrys.com>; 2009.
[23] Abdelghany AM, Mekhail MS, Abdelrazek EM, Aboud MM. Combined DFT/FTIR structural studies of monodispersed PVP/gold and silver nano particles. J Alloys Compd 2015;646:326–32.
[24] Kessi A, Delley B. Density functional crystal vs. cluster models as applied to zeolites. Int J Quantum Chem 1998;68:135–44.
[25] Bertoli AC, Carvalho R, Freitas MP, Ramalho TC, Mancini DT, Oliveira MC, et al. Theoretical spectroscopic studies and identification of metal-citrate (Cd and Pb) complexes by ESI-MS in aqueous solution. Spectrochim Acta A 2015;137:271–80.
[26] Matveev A, Staufer M, Mayer M, Rösch N. Density functional study of small molecules and transition-metal carbonyls using revised PBE functionals. Int J Quantum Chem 1999;75:863–73.
[27] Hawkey PM, Lewis DA. Medical bacteriology – a practical approach. United Kingdom: Oxford University Press; 1994. p. 181–94.
[28] Mosmann T. Rapid colorimetric assay for cellular growth and survival: application to proliferation and cytotoxicity assays. J Immunol Methods 1983;65:55–63.
[29] Lissi E, Modak B, Torres R, Escobar J, Urzua A. Total antioxidant potential of resinous exudates from Heliotropium species, and a comparison of the ABTS and DPPH methods. Free Radical Res 1999;30:471–7.
[30] El-Gazzar A, Youssef M, Youssef A, Abu-Hashem A, Badria F. Design and synthesis of azolopyrimidoquinolines, pyrimidoquinazolines as anti-oxidant, anti-inflammatory and analgesic activities. Eur J Med Chem 2009;44:609–24.
[31] Aeschlach R, Loliger J, Scott C, Murcia A, Butler J, Halliwell B, et al. Antioxidant actions of thymol, carvacrol, 6-gingerol, zingerone and hydroxytyrosol. Food Chem Toxicol 1994;32:31–6.
[32] Denizot F, Lang R. Rapid colorimetric assay for cell growth and survival. J Immunol Methods 1986;89:271–7.
[33] Mauceri H, Hanna N, Beckett M, Gorski D, Staba M, Stellato K, et al. Combined effects of angiostatin and ionizing radiation in antitumour therapy. Nature 1998;394:287–91.
[34] Morimoto Y, Tanaka K, Iwakiri Y, Tokuhiro S, Fukushima S, Takeuchi Y. Protective effects of some neutral amino acids against hypotonic hemolysis. Biol Pharm Bull 1995;18:417–1422.
[35] Ibrahim K, Gabr I, Abu El-Reash G, Zaky R. Spectral, magnetic, thermal, antimicrobial, and eukaryotic DNA studies on acetone [N-(3-hydroxy-2-naphthoyl)] hydrazone complexes. Monatsh Chem 2009;140:625–32.
[36] Ibrahim K, Zaky K, Gomma E, El-Hady M. Spectral, magnetic, thermal studies and antimicrobial activity of (E)-3-(2-benzylidenehydrazinyl)-3-oxo-N-(thiazol-2-yl) propanamide complexes. Res J Pharm Biol Chem Sci 2011;2:391–404.
[37] Pretsch E, Bühlmann P, Badertscher M. Structure determination of organic compounds. 4th ed. Berlin, Heidelberg: Springer Science & Business Media; 2009.
[38] Zaky R. Synthesis, characterization, antimicrobial, and genotoxicity activities of acetoacetanilide-4-ethyl thiosemicarbazone complexes. Phosphorus Sulfur Silicon 2011;186:365–80.
[39] Zaky R, Yousef T. Spectral, magnetic, thermal, molecular modelling, ESR studies and antimicrobial activity of (E)-3-(2-(2-hydroxybenzylidene) hydrazinyl)-3-oxo-n (thiazole-2-yl) propanamide complexes. J Mol Struct 2011;1002:76–85.
[40] Cotton FA, Wilkinson G, Murillo CA, Bochmann M. Advanced inorganic chemistry. 6th ed. New York: John Wiley & Sons Inc.; 2003.
[41] Zalaoglu Y, Ulgen A, Terzioglu C, Yildirim G. Theoretical study on the characterization of 6-methyl 1,2,3,4-tetrahydroquinoline using quantum mechanical calculation methods. Fen Bilimleri Dergisi 2010;14:66–76.
[42] Tanak H, Köysal Y, Işık Ş, Yaman H, Ahsen V. Experimental and computational approaches to the molecular structure of 3-(2-Mercaptopyridine)phthalonitrile. Bull Korean Chem Soc 2011;32:673–80.
[43] Filipović N, Borrmann H, Todorović T, Borna M, Spasojević V, Sladić D, et al. Inorganica Chim Acta 2009;362:1996–2000.
[44] Thimmaiah N, Chandrappa T, Jayarama R. Structural studies of biologically active complexes of zinc(II), cadmium(II), mercury(II) and copper(II) with p-anisaldehyde thiosemicarbazone. Polyhedron 1984;3:1237–9.
[45] Nagar R. Syntheses, characterization, and microbial activity of some transition metal complexes involving potentially active O and N donor heterocyclic ligands. J Inorg Biochem 1990;40:349–56.
[46] Johari RB, Sharma RC. J Indian Chem Soc 1988;65:793–4.
[47] Abd El-Wahab Z, El-Sarrag M. Derivatives of phosphate Schiff base transition metal complexes: synthesis, studies and biological activity. Spectrochim Acta A 2004;60:271–7.
[48] Panchal P, Parekh H, Patel M. Preparation, characterization and toxic activity of oxovanadium(IV) mixed ligand complexes. Toxicol Environ Chem 2005;87:313–20.
[49] Kostova I, Saso C. Advances in research of Schiff-base metal complexes as potent antioxidants. Curr Med Chem 2013;0:4609–32.
[50] Yousef A, Badria F, Ghazy S, El-Gammal O, Abu El-Reash G. In vitro and in vivo antitumor activity of some synthesized 4-(2-pyridyl)-3-Thiosemicarbazides derivatives. J Med Med Sci 2011;3:37–46.

[51] Ghazy SE, Samra SE, Mahdy AF, El-Morsy SM. Removal of aluminum from some water samples by sorptive-flotation using powdered modified activated carbon as sorbent and oleic acid as surfactant. Anal Sci 2006;22:377–82.
[52] Klassen VI, Mokrousov VA. An introduction to the theory of flotation. London: Butterworths; 1963.
[53] Ghazy SE, Mostafa GA. Flotation-separation of chromium(VI) and chromium(III) from water and leathers tanning waste using active charcoal and oleic acid surfactant. Bull Chem Soc Jpn 2001;74:1273–8.
[54] Ghazy SE, Kabil MA. Determination of trace copper in natural waters after selective separation by flotation. Bull Chem Soc Jpn 1994;67:474–8.
[55] Ghazy SE, Rakha TH, El-Kady EM, El-Asmy AA. Use of some hydrazine derivatives for the separation of mercury(II) from aqueous solutions by flotation technique. Indian J Chem Techn 2000;7:178–82.
[56] Pol'kin SI, Berger GS, Revazashavili IB, Shchepkina MM. Phase diagram and collector properties of oleic acid with changing pH. Izv Vyssh Ucheb Zaved Tsvet Met 1968;11:6–11.
[57] Ramachandra RS. Surface chemistry of froth flotation, reagents and mechanisms, vol. 2. 2nd ed. New York: Kluwer Academic/Plenum Publishers; 1982.